Available online at www.sciencedirect.com
SCIENCE DIRECT®

Journal of the European Ceramic Society 24 (2004) 1313–1317

www.elsevier.com/locate/jeurceramsoc

# Oxygen permeability of gadolinium-doped ceria at high temperature

Hee Jung Park, Gyeong Man Choi*

*Department of Materials Science and Technology, Pohang University of Science and Technology, san 31, Hyoja-dong, Pohang, 790-784, South Korea*

**Abstract**

The oxygen permeability and the electrical conductivity of gadolinium-doped ceria, $Ce_{0.8}Gd_{0.2}O_{2-\delta}$ (GDC20) was measured as a function of temperature (1400–1600 °C) and oxygen partial pressure (0.21–$10^{-10}$ atm). The measured oxygen permeation was compared with that estimated from the electrical conductivity. The oxygen permeation driven by a oxygen potential gradient, in the absence of an applied electrical potential, was measured by an oxygen sensor. The results of electrical conductivity measurement show that the doped-ceria is a mixed electronic and oxygenionic conductor at high temperature, guaranteeing the high oxygen permeability. The oxygen permeability of this compound is more than two orders of magnitude higher than that of Ca-doped $ZrO_2$ in high $Po_2$ region. The comparison of oxygen permeation and electrical conductivity shows that the measured permeation is less than the expected value estimated from the electrical conductivity. The deviation was ascribed to the polarization effect.


*Keywords:* Electronic conductivity; GDC; Ionic conductivity; Oxygen permeability

## 1. Introduction

Oxygen permeating ceramics with mixed ionic and electronic conductivity have received much interest for high temperature applications such as oxygen separation, the production of CO and $H_2$ (fuel gases), and oxygen removal from steel melt.[1,2] The conditions required for deoxidizing steel melt are chemical and thermal stability in addition to high oxygen permeability. Although $ZrO_2$ doped with divalent or trivalent ions shows the required stability, its oxygen permeability is low due to the low mixed conductivity.[3] Thus, $ZrO_2$ doped with metal oxides has been tested to induce high electronic conductivity.[4]

Doped $CeO_2$ is known as an oxygen ion conductor with the same structure as zirconia, i.e., a fluorite structure.[5] However, it shows high electronic conductivity in addition to the high oxygen ionic conductivity due to the reduction of the cerium ion from the tetravalent to the trivalent state at high temperatures in a reducing atmosphere.[6] Most research[5,7] mainly concern the electrical conductivities at low temperatures due to its possible use as a solid electrolyte. The oxygen permeability at high temperature (>1400 °C) has scarcely been studied for acceptor-doped $CeO_2$, especially in low $Po_2$.

In this study, the oxygen permeability of $Ce_{0.8}Gd_{0.2}O_{2-\delta}$ (GDC20) under a high potential gradient was investigated at high temperature. The oxygen permeability was compared with the value estimated from the electrical conductivity data.

## 2. Experimental procedure

$CeO_2$ and $Gd_2O_3$ (both 99.9%, from High Purity Chemicals, Japan) were mixed in ethyl alcohol while milling with alumina balls for 12 h. The mixed powder was calcined at 1200 °C for 2 h in air, ground and pressed into a pellet, followed by cold isostatic pressing (CIP) at 200 MPa. The pressed pellet was sintered at 1650 °C for 4 h in air.

For the four-probe d.c. conductivity measurement, a rectangular bar-shaped sample ($3\times2\times18mm^3$) was cut from sintered pellets. Four notches were cut for electrode-wire winding and Pt wires (0.2 mm) were tightly wound on the Pt-pasted (Engelhard model #6926) notches. The direct current was supplied by current source (Keithley, K220, USA) and the voltage difference was detected by a multimeter (Keithley). The oxygen partial pressure ($Po_2$) dependence of electrical conductivity was measured in the temperature range of 1100–1400 °C.

* Corresponding author. Tel.: +82-562-279-2146; fax: +82-562-279-2399.
*E-mail address:* gmchoi@postech.ac.kr (G.M. Choi).

0955-2219/$ - see front matter © 2003 Elsevier Ltd. All rights reserved.
doi:10.1016/S0955-2219(03)00555-7

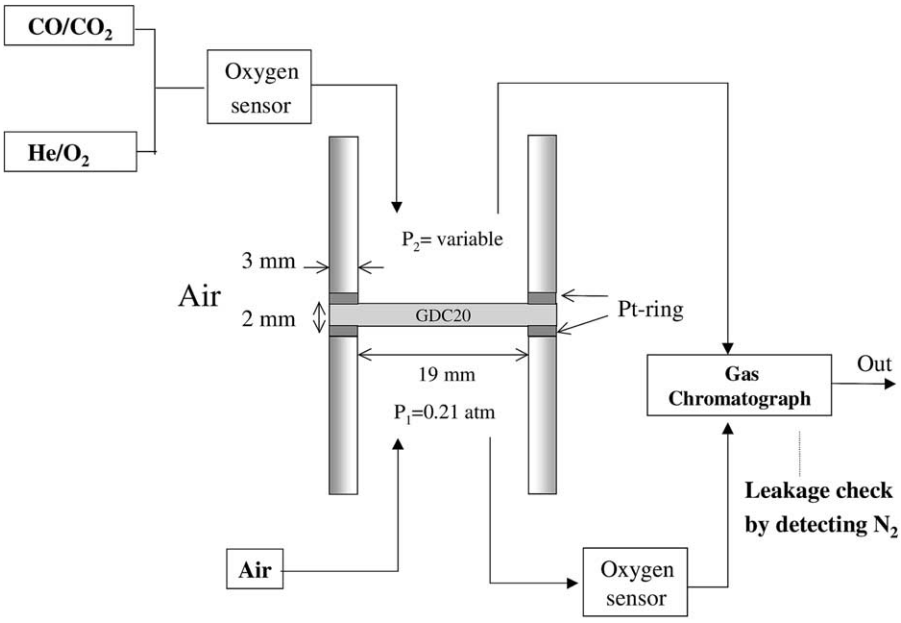


Fig. 1. Schematic diagram of oxygen-permeation measurement system for $Ce_{0.8}Gd_{0.2}O_{2-\delta}$ (or GDC20).

The $Po_2$ (1–$10^{-11}$ atm) was controlled with $He/O_2$ or $CO/CO_2$ gas mixtures.

Fig. 1 shows a schematic diagram of the oxygen permeation measurement system. The sintered ceria pellet with 25 mm diameter was cut at a thickness of 2 mm. The sample was sandwiched and pressed between two alumina support tubes. Pt-rings were used as sealant. The permeation measurement was performed in the temperature range 1400–1600 °C. The $Po_2$ at the feed side was fixed by air ($P_1 = 0.21$ atm), while the $Po_2$ at the permeate side was controlled by changing the $He/O_2$ or $CO/CO_2$ ratios ($P_2 = 0.21$–$10^{-10}$atm). The gas flow rate was 100 ml/min at both feed and permeate sides. Gas leakage through the side of the sample was detected by monitoring the nitrogen concentration using a gas chromatograph (HP 4890D, USA). The amount of nitrogen was below 0.02% of the helium gas volume (100 ml/min) which is negligible to the permeated oxygen flux.

The oxygen flux ($Jo_2$) was calculated by analyzing the oxygen concentration ($Co_2$) at the feed side using a zirconia oxygen sensor,

$$Jo_2\left[\mathrm{ml/min \cdot cm^2}\right] = \frac{F[\mathrm{ml/min}] \cdot Co_2[\mathrm{vol.fraction}]}{A[\mathrm{cm^2}]} \quad (1)$$

where $F$ is the flow rate, and $A$ is the area of permeation.

## 3. Results and discussion

The $Po_2$ dependence of the total electrical conductivity between 1100 and 1400 °C, measured by a four-probe d.c. method, is shown in Fig. 2. The plot of log $\sigma$ versus log $Po_2$ can be divided into two regions. In the high $Po_2$ region, the conductivity is nearly independent of $Po_2$. In this region, the ionic conductivity is dominant due to the Gd-acceptor doping for Ce site. This doping reaction can be written as, using the Kröger and Vink notation:

$$Gd_2O_3 \overset{2CeO_2}{\rightarrow} 2Gd'_{Ce} + 3O^x_o + V''_o. \quad (2)$$

The ionic conductivity, independent on $Po_2$, is given by

$$\sigma_i = \frac{A_0}{T}\exp(-E_a/kT) \quad (3)$$

where $A_0$ is the pre-exponential factor, and $E_a$ is the activation energy.

In the low $Po_2$ region, the total conductivity increases with decreasing $Po_2$ due to the electronic conduction. The occurrence of electronic conductivity in doped $CeO_2$ is well known in the reduced condition.[6] The equilibrium reaction which contributes to the electronic conduction is

$$Oo^x \rightarrow \frac{1}{2}O_2(g) + V''_O + 2e'. \quad (4)$$

In this reaction, the electronic defect (e′) is due to the Ce reduction ($Ce^{4+} \rightarrow Ce^{3+}$). The electronic conductivity ($\sigma_e$) is dependent on $Po_2^{-1/4}$ when the oxygen vacancy concentration is fixed by Gd doping as shown by Eq. (2).

Thus the total conductivity ($\sigma_t$) can be expressed by the sum of ionic ($\sigma_i$) and electronic ($\sigma_e$) conductivity.

$$\sigma_t = \sigma_i + \sigma_e^o Po_2^{-1/4}. \quad (5)$$

In Fig. 2, the dotted lines indicate the experimental results best-fitted by using Eq. (5). It is shown that the results agree nicely with the defect model. The ionic and electronic conductivities obtained by the fitting data are given by

$$\sigma_i = \frac{1.70 \times 10^5}{T} \exp\left(-\frac{0.72 \pm 0.01eV}{kT}\right) \quad (6)$$

$$\sigma_e = 4.28 \times 10^5 \exp\left(-\frac{2.28 \pm 0.03eV}{kT}\right) Po_2^{-1/4}. \quad (7)$$

These results are in good agreement with the low temperature data (<1000 °C).[5,8]

The deviation of the conductivity curve from the simple model [Eq. (5)] in more reducing conditions at 1400 °C is due to the formation of additional oxygen vacancies generated by the reduction that leads to the decrease of the ionic conductivity as similarly shown for $Ce_{0.8}Y_{0.2}O_{2-\delta}$.[6]

Oxygen permeability ($Jo_2L$) of GDC20 at different temperatures as a function of permeate side $Po_2$ ($P_2$) is shown in Fig. 3, where $L$ is the membrane thickness. The rate of oxygen permeation is generally limited by two factors. One factor is the solid-state diffusion through the membrane and the other is the surface exchange kinetics of the membrane. For this compound, it is reported that the surface exchange kinetics are faster than the oxygen self-diffusion above 900 °C.[9] Thus oxygen flux is limited by the bulk diffusion, expressed by the following Wagner equation:

$$Jo_2 \cdot L = \frac{RT}{4^2F^2} \int_{P_2}^{P_1} \frac{\sigma_i\sigma_e}{\sigma_e + \sigma_i} d\ln Po_2. \quad (8)$$

If none of the ionic and the electronic conductivities is negligible, this equation can be rearranged for GDC20 using Eq. (5) as following:

$$Jo_2 \cdot L = \frac{RT\sigma_i}{4F^2} \left[\ln \frac{1}{\sigma_i + \sigma_e^o P_{O_2}^{-1/4}}\right]_{P_2}^{P_1}. \quad (9)$$

Eq. (9) tells us that the oxygen permeability can be estimated if we know both the electronic and the ionic conductivities. The dotted lines in Fig. 3 show the estimated flux using Eq. (9).

Three regions can be distinguished in Fig. 3. In region 1, the oxygen potential difference between the two sides of the membrane is small and the measured data agree well with the estimated values. However, in region 2, the measured data begin to deviate from the dotted lines and the deviation becomes severe with decreasing permeate-side $Po_2$. The reason for the deviation may originate from the polarization effect as explained in the following. The $Po_2$ values of permeate-side gas ($P_2$) and that on the membrane surface are not equal. Permeation rate decreases as the immediate surface of the membrane has a higher $Po_2$ than that in permeate-side gas. When this occurs, the gas–solid mass-transfer depends on the flow rate of feed and permeate sides[11] as observed in this experiment. In region 3, the deviation from the dotted lines becomes nearly constant with further decreases in permeate-side $Po_2$. It implies that the similar $Po_2$ gradient is maintained between the membrane surface and the flowing gas once $P_2$ drops below a certain value. The measured flux values are approximately 1/3 of the estimated values in this region. The polarization effect was also observed by Fouletier et al.[10] for zirconia.

In Fig. 4, the estimated oxygen partial pressure ($P_e$) on the membrane surface of the permeate-side was

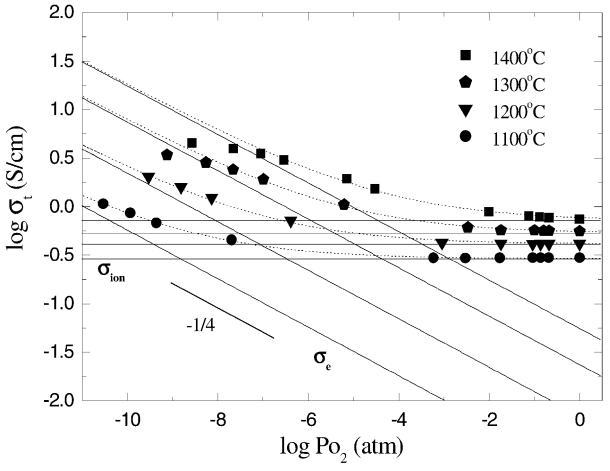


Fig. 2. Electrical conductivities as a function of $Po_2$ for $Ce_{0.8}Gd_{0.2}O_{2-\delta}$ at different temperatures.

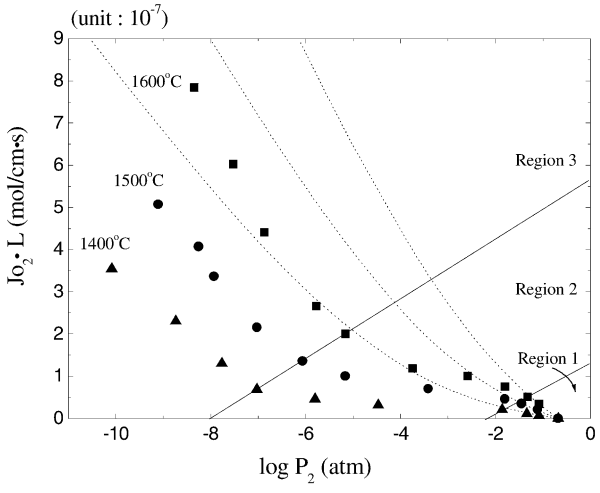


Fig. 3. Oxygen permeability as a function of $Po_2$ for $Ce_{0.8}Gd_{0.2}O_{2-\delta}$ at high temperatures. The dotted lines are the estimated values from the conductivities.

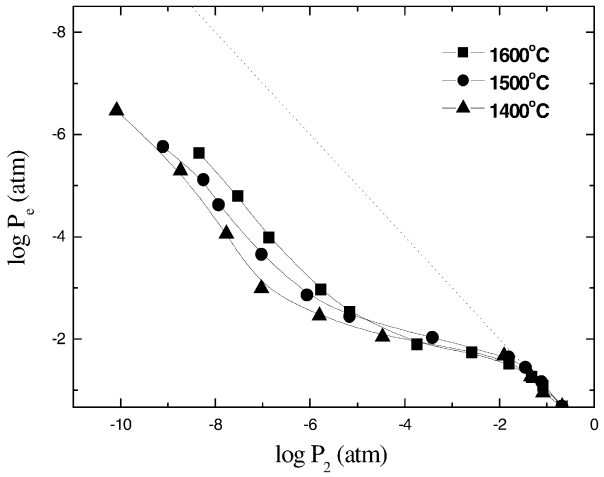


Fig. 4. The estimated oxygen partial pressure ($P_e$) on the membrane surface of permeate side $Po_2$. The dotted line is for $P_e = P_2$.

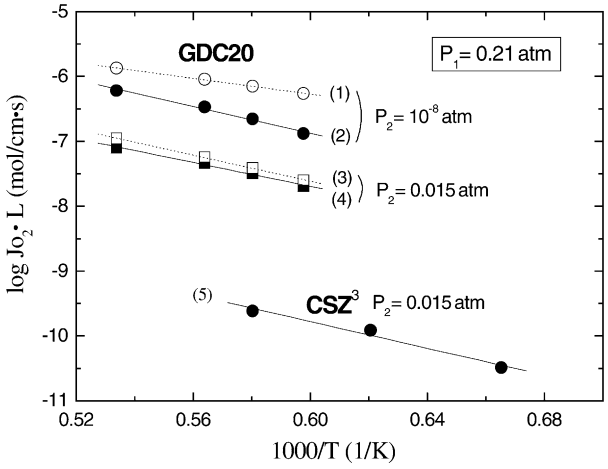


Fig. 5. Temperature dependence of the oxygen permeability of GDC20 for (1) $P_2 = 10^{-8}$ atm and (3) $P_2 = 0.015$ atm, estimated from the conductivity data using Eq. (9), and that of measured data for (2) $P_2 = 10^{-8}$ atm and (4) $P_2 = 0.015$ atm. The permeability of calcia-stabilized zirconia for $P_2 = 0.015$ atm was also shown for comparison. $P_1$ was 0.21 atm for all data.

shown at different temperatures. For a given permeate-side $Po_2$ ($P_2$), the measured flux is lower than the value estimated from the conductivity data. The reduction in flux is due to the higher $Po_2$ ($P_e$) on the membrane surface than that in the gas flow. The permeated oxygen molecules file up on the membrane surface before moving into the gas phase and thus reduce the oxygen potential gradient. As shown in Fig. 4, the difference between log $P_e$ and log $P_2$ is maintained approximately as the constant value. For highest $Po_2$ (log $P_2 < -2$), the difference between $P_e$ and $P_2$ is small. In other words, the polarization effect is small if the $Po_2$ gradient between $P_1$ and $P_2$ is small. For high $P_2$ region ($10^{-2}$–$10^{-5}$ atm), the polarization effect increases but it is little different with temperature. However, for the low $P_2$ region ($< 10^{-5}$ atm), the effect is the highest at 1400 °C. In other words, the difference between log $P_e$ and log $P_2$ is largest at this temperature.

The temperature dependence of the oxygen permeability of GDC20 was shown in Fig. 5. Since the oxygen permeability ($Jo_2 \cdot L$) is the activated process, it can be shown as the following Arrhenius equation.

$$Jo_2 \cdot L = J_o \exp\left(-\frac{E_a}{kT}\right) \quad (10)$$

where $E_a$ is the apparent activation energy.

When the $Po_2$ gradient is small, for example, $P_1 = 0.21$ atm and $P_2 = 0.015$ atm, the apparent activation energy ($E_a = 1.84$ eV) of the measured permeation is only slightly smaller than that ($E_a = 1.97$ eV) estimated from the conductivity data. Thus the oxygen permeation of GDC20 is apparently limited by bulk diffusion for the small oxygen potential gradient. The activation energy is slightly smaller than that of the electronic conduction [2.28 eV in Eq. (6)]. This is expected since the rate limiting process is the minority electron movement in high $Po_2$ region. When the $Po_2$ gradient is large, for $P_2 = 10^{-8}$ atm, the activation energy is 2.05 eV, much larger than that estimated value of 1.22 eV. While the estimated $E_a$ is close to that of ionic conduction as expected, the high measured $E_a$ value is due to the temperature-dependent polarization effect as shown in Fig. 4. Since, in the low $Po_2$ region, the oxygen ions are minority charge carriers and the minority carrier movement is rate limiting, the $E_a$ for oxygen conduction was expected. In Table 1, the activation energies obtained from the conductivity and permeation measurements are shown.

Table 1
The activation energies obtained from the conductivity and the permeation measurements. $P_1$ (feed side) is 0.21 atm for the permeation measurement

| Method | | | Activation energy (eV) |
|---|---|---|---|
| 4-probe d.c. | | Ionic conductivity ($\sigma_i$) | 0.72±0.01 |
| | | Electronic conductivity ($\sigma_e$) | 2.28±0.03 |
| Permeation | $Jo_2 \cdot L$ | $P_2 = 0.015$ atm | 1.84±0.06 |
| | | $P_2 = 10^{-8}$ atm | 2.05±0.08 |

The oxygen permeability of GDC20 is about two orders of magnitude higher than that of $Zr_{0.849}Ca_{0.151}O^{3}_{2-\delta}$ as show in Fig. 5.

## 4. Conclusions

The total conductivity of GDC20 was measured in a wide range of $Po_2$ at high temperatures. The conductivity curves were fitted with the $Po_2$-independent ionic conductivity and the $Po_2^{-1/4}$ dependent electronic conductivity. The activation energy of ionic and electronic

conductivities are 0.72 and 2.28 eV, respectively. The expected oxygen permeability was calculated using the measured electrical conductivity values. The measured oxygen permeability was in good agreement with that estimated from the electrical conductivity in the high-permeate $Po_2$ region, however, it deviated from the expected value with decreasing $Po_2$ due possibly to the polarization effect. The oxygen permeability of this compound was about two orders of magnitude higher than that of Ca-doped $ZrO_2$.[3] In order to determine the rate-limiting step more clearly, the oxygen flux with varying sample thicknesses or surface treatments needs to be measured.

## Acknowledgements

The authors are grateful for the financial support from POSCO, Korea.

## References

1. Balachandran, U., Dusek, J. T., Mieville, R. L., Poeppel, R. B., Kleefisch, M. S., Pei, S., Kobylinski, T. P., Udovich, C. A. and Bose, A. C., Dense ceramic membrane for partial oxidation of methane to syngas. *Applied Catal. A General*, 1995, **133**, 19–29.
2. Yuan, S., Pal, U. and Chou, K. C., Modeling and scaleup of galvanic deoxidation of molten metals using solid electrolyte cells. *J. Am. Ceram. Soc.*, 1996, **79**, 641–650.
3. Dou, S. and Masson, C. R., Mechanism of oxygen permeation through lime-stabilized zirconia. *J. Electrochem. Soc.*, 1985, **132**, 1843–1849.
4. Arashi, H. and Naito, H., Oxygen permeability in $ZrO_2$–$TiO_2$–$Y_2O_3$ system. *Solid State Ionics*, 1992, **53-56**, 431–435.
5. Kudo, T. and Obayashi, H., Mixed electrical conduction in the fluorite-type $Ce_{1-x}Gd_xO_{2-x/2}$,. *J. Electrochem. Soc.*, 1976, **123**, 415–419.
6. Cales, B. and Baumard, J. F., Transport properties and defect structure of nonstoichiometric yttria doped ceria. *J. Phys. Chem. Solids*, 1984, **45**, 929–935.
7. Wang, S., Kobayashi, T., Dokiya, M. and Hashimoto, T., Electric and ionic conductivity of Gd-doped ceria. *J. Electrochem. Soc.*, 2000, **147**, 3606–3609.
8. Steele, B., Appraisal of $Ce_{1-y}Gd_yO_{2-y/2}$ electrolytes for IT-operation at 500 °C. *Solid State Ionics*, 2000, **129**, 95–110.
9. Lane, J. A. and Kilner, A. J., Oxygen surface exchange on gadolinia doped ceria. *Solid State Ionics*, 2000, **136-137**, 927–932.
10. Fouletier, J., Fabry, P. and Kleitz, M., Electrochemical semipermeability and the electrode microsystem in solid oxide electrolyte cells. *J. Electrochem. Soc.*, 1976, **123**, 204–212.
11. Stephens, W. T., Mazanec, T. J. and Anderson, H. U., Influence of gas flow rate on oxygen flux measurements for dense oxygen conducting ceramic membranes. *Solid State Ionics*, 2000, **129**, 271–284.